Int. J. Heat Mass Transfer. Vol. 34, No. 9, pp. 2219–2230, 1991
Printed in Great Britain

0017–9310/91 $3.00+0.00
Pergamon Press plc

On the steady-state performance of natural circulation loops

P. K. VIJAYAN and S. K. MEHTA
Reactor Group, Bhabha Atomic Research Centre, Trombay, Bombay 400085, India

and

A. W. DATE
Department of Mechanical Engineering, Indian Institute of Technology, Powai, Bombay 400076, India

(*Received* 19 *January* 1989 *and in final form* 18 *July* 1990)

Abstract—This paper reports a comparison between natural and forced circulation data in a figure-of-eight loop relevant to a pressure tube type heavy water reactor. It is shown that both friction and heat transfer are affected by the presence of buoyancy induced secondary flows under steady-state natural circulation conditions. Several past proposals for correlating the overall hydraulic loss coefficient are reviewed and a generalized correlation is proposed that is non-loop specific. The correlation successfully predicts experimental data from three different loops. The experimental data, however, are generated with seven different geometric configurations of these three loops.

1. INTRODUCTION

IN A NATURAL circulation loop the fluid circulation is maintained by the buoyancy force caused by density gradients. Such loops find applications in nuclear reactor core cooling, solar water heaters, geothermal processes, transformer cooling and cooling of certain types of internal combustion engines and rotating machinery. General reviews on natural circulation loops are given by Japikse [1], Zvirin [2], Mertol and Greif [3, 4] and Greif [5]. Among loop thermosyphons, often a distinction is made between closed-loop and open-loop systems. Closed-loop thermosyphons have at least one heat source and one heat sink connected by pipes. Open-loop thermosyphons, on the other hand, need to have only a heat source with its inlet and outlet connected to the same or two separate reservoirs.

Many geometric configurations of closed-loop thermosyphons have been studied. The simple geometry loops studied are the rectangular [6–12] and the toroidal [13–15] thermosyphons. The simple geometry loops often have uniform pipe diameter throughout the loop. More complicated loops having varying pipe diameters at different segments have also been investigated in the context of nuclear reactors [16–22]. Studies on the open-loop thermosyphons are limited. Bau and Torrance [23] performed experiments with a vertical U-shaped open loop connected to an isothermal reservoir. A horizontal U-shaped open loop thermosyphon was investigated by Haware *et al.* [24].

An important requirement for the design of natural circulation loops is an experimentally validated theoretical model to predict the natural circulation flow rate and temperatures for a loop having specified geometry and operating conditions. Most of the theoretical analyses to date are based on the one-dimensional approach which requires the friction factor, loss coefficients and heat transfer coefficients to be provided as input. Usually forced flow correlations are assumed to be applicable for natural circulation flow in these analyses. Proper comparison of the forced flow and natural circulation correlations are, however, not reported so far. For example, in the case of friction, the reported comparisons [13, 23] are between the measured natural circulation friction factor and that predicted using the forced flow correlations applicable to fully developed flow. In a closed loop, however, due to flow area changes, the presence of bends, etc., the flows are often not fully developed. Therefore, a realistic comparison can only be made by measuring both the natural circulation and the forced flow friction factors for the loop under investigation. Again, such comparisons have not been reported so far.

Secondly, although a large number of experiments [6–27] on natural circulation loops have been reported in the literature, comparison with theory is lacking. Even where such comparisons are presented [8, 9, 17, 25, 26, 28] the parameters chosen for comparison are either dimensional or loop-specific non-dimensional groups. This makes it difficult to compare data from different loops and to extend data from small-scale to large-scale loops.

The two-fold purpose of the present contribution is therefore:

NOMENCLATURE

A	cross-sectional area
A_{hc}	heater surface area
C_p	specific heat
D_{hc}	heater hydraulic diameter
g	gravity acceleration
Gr	Grashof number, $D^3\rho^2\beta g(T_b - T_w)$
Gz	Graetz number, $Re\,Pr(\pi D/4L)$
h	heat transfer coefficient
k	thermal conductivity
K	loss coefficient
Nu	Nusselt number
ΔP_t	total pressure loss in the loop
Re	Reynolds number, $DW/A\mu$
T	temperature
W	mass flow rate
Z	elevation.

Greek symbols

β	thermal expansion coefficient
μ	dynamic viscosity
ρ	density.

Subscripts

b	bulk
c	cooler
cl	cold leg
cor	forced flow correlations
f	forced flow experiment
h	heater
hl	hot leg
i	inside
m	mean
nc	natural circulation
s	secondary side of cooler
si	secondary inlet
w	wall.

(1) To measure and compare the friction and the heat transfer coefficients in a closed loop under natural circulation and forced flow conditions; where the forced flow rates are comparable in magnitude to those prevailing during natural circulation. The closed loop in which measurements are made is a figure-of-eight loop.

(2) To present a generalized correlation for the effective pressure-loss coefficient that is found to be applicable to several loops of different dimensions and geometry. The generalized correlation uses such parameters that makes it non-loop specific and allows prediction of mass flow rates from the known independent parameters of the loop.

2. EXPERIMENTAL LOOP

The experimental loop (see Fig. 1) consisted of two horizontal heaters of annular geometry, with the inner tube directly heated by electric current. The heaters were connected to headers and the headers were connected to vertical inverted U-tube coolers by small diameter tubes. Each cooler (tube-in-tube type) consisted of an inverted glass U-tube, the vertical portions of which were cooled by water flowing in the surrounding annulus formed with another glass tube. The system pressure was maintained at near atmospheric by a small expansion tank provided at the highest elevation. The loop was insulated using precast asbestos magnesia.

There were 24 thermocouples installed at various points in the loop (see Fig. 1) to measure the heater surface and water temperatures. All thermocouples were connected to a datalogger which could scan all the channels in less than 2 s. The power input to the heater was obtained as the product of voltage and current which were measured. The secondary side flow rates to the individual coolers were measured with the help of two rotameters. The water temperatures at the inlet and outlet of both the coolers were also measured. The loop had a small pump which was used to establish a steady forced flow, when required. A magnetic flow meter was employed to measure this forced flow.

The loop was used to generate data under natural and forced circulation conditions under varying conditions of the heater power (Q_h) and the secondary flow rate (W_s). From the data generated, it was possible to calculate the effective hydraulic loss coefficient and the heat transfer coefficients at the cooler and the heater during natural circulation and forced flow conditions. These will be discussed after development of the mathematical formulation in the next section.

3. PARAMETERS OF INTEREST AND CORRELATIONS

3.1. *Parameters of interest*

Under steady-state conditions in a natural circulation loop, when the buoyancy and frictional forces are in perfect balance, it can be easily shown [2] that

$$W = [p\rho_m^2\beta g Q_h Z_m A_c^2/(K_{eff}C_p)]^{1/3} \tag{1}$$

where p is a known integer constant (see Table 1 for values of p for loops of different geometry) and Z_m is the appropriate elevation difference between the cooler and the heater

$$Z_m = (1/\Delta T_h)\oint T(Z)\,dZ. \tag{2}$$

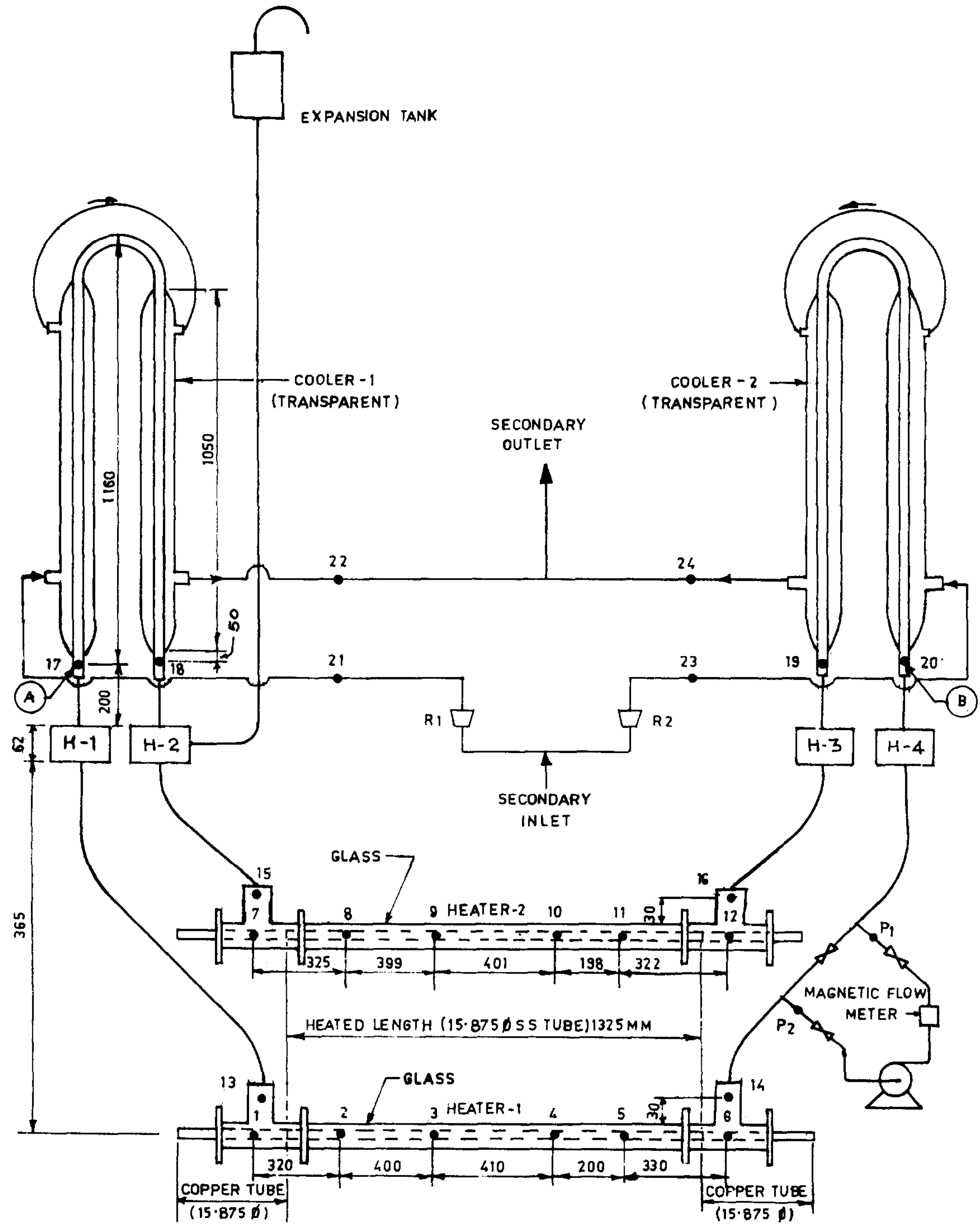

LEGEND

1----22 THERMOCOUPLE NUMBERS.

●—THERMOCOUPLE LOCATIONS

R1, R2 ROTA METERS

P_1 , P_2 PRESSURE TAPS

H-1, H-2, H-3, H-4 HEADERS

Ⓐ Ⓑ----DYE INJECTION POINTS

Fig. 1. Experimental loop.

Table 1. Value of constant p in equation (1)

Serial No.	Type of loop	Examples	p	References
1	Rectangular loop	Loops relevant to pressurized water reactors, solar water heaters, etc.	2	[9, 16, 17, 19, 23]
2	Toroidal loop	Loop employed in refs. [13, 34]	2	[13, 34]
3	Figure-of-eight loop	Loops relevant to pressurized heavy water reactors	4	[20] and present study

Hallinan and Viskanta [11], for a loop consisting of a vertical heater and a vertical cooler of equal length, L, defined a driving temperature difference ΔT_D as

$$\Delta T_D = (1/L)\oint T(Z)\,dZ. \quad (2a)$$

For a general case, however, where the heaters may be horizontal or even inclined, equation (2), which defines Z_m rather than a representative driving temperature difference, is more appropriate.

If the fluid temperature in the heater and the cooler is assumed to vary linearly with Z, then it can be shown that Z_m equals the centreline elevation difference between the cooler and the heater. In the thermosyphon analysis, such an assumption is usually made [12].

The overall loss coefficient, K_{eff}, can be defined in two ways

$$K_{eff} = \sum(4f_iL_i/D_i + K_i) \quad (3a)$$

$$= \Delta P_l/(\rho_m u^2/2) \quad (3b)$$

where f_i, L_i, D_i and K_i in equation (3a) are the fully developed friction factor, length, diameter and the form loss coefficient, respectively, of the ith segment and u is the bulk fluid velocity in any segment for the loop. With respect to the cooler cross-sectional area, for example

$$u = W/(\rho_m A_c). \quad (4)$$

Thus W can be predicted from equation (1) if K_{eff} is specified by correlations or from experiment. The loop temperatures T_{hl} and T_{cl} can be predicted if the overall heat transfer coefficient, U_c, for the cooler is specified from correlations or experiment. Similarly the heater temperature, T_h, can be predicted from

$$Q_h = (Nu_h\,kA_{hc}/D_{hc})[\bar{T}_h - \bar{T}_b] \quad (5)$$

where bars over T_h and T_b represent average values in the heater and Nu_h must be specified.

3.2. *Correlations from the present experiment*

From the present experiments with the figure-of-eight loop, correlations for K_{eff}, Nu_c $(= U_cD_c/K)$ and Nu_h were determined under natural circulation conditions. These correlations are

$$K_{eff,nc} = 38\,440/Re_c^{0.635} \quad (6)$$

$$Nu_{c,nc} = 1.94Re_c^{0.164} \quad (7)$$

and

$$Nu_{h,nc} = 0.067Re_h^{0.8}. \quad (8)$$

By applying the conventional forced flow correlations for friction factor ($f = 16/Re$) and loss coefficient [29, 30] to different segments of the loop, the corresponding correlations for the above parameters were found to be

$$K_{eff,cor} = 2.55\times10^5/Re_c. \quad (9)$$

Similarly the relevant heat transfer correlations for the cooler [29] and the annular heater [31] can be given by

$$Nu_{c,cor} = \frac{3.66(1+0.047Gz^{2/3})+0.085Gz}{1.62(1+0.047Gz^{2/3})+0.0144Gz} \quad (10)$$

$$Nu_{h,cor} = 0.1135Re_h^{0.45}\,Pr^{0.5}\,Gr^{0.05}. \quad (11)$$

In addition, the present loop, as mentioned in Section 2, was also run under forced flow conditions with flow rates comparable to those estimated under natural circulation conditions. Thus a correlation for K_{eff} could be determined under forced flow conditions and was found to be

$$K_{eff,f} = 2.68\times10^5/Re_c^{0.964}. \quad (12)$$

It will be instructive to investigate the merits of the forced flow correlations in relation to the natural circulation correlations. Figure 2 presents the measured variation of K_{eff} with Re_c under both natural and forced flow conditions. Also plotted in the figure are

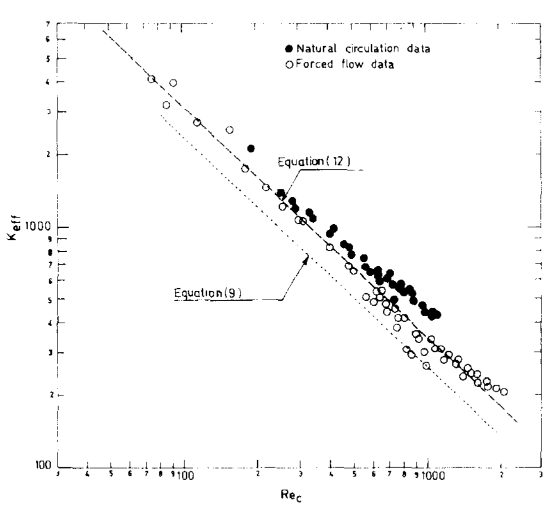

FIG. 2. The effective hydraulic loss coefficient for forced and natural circulation flow.

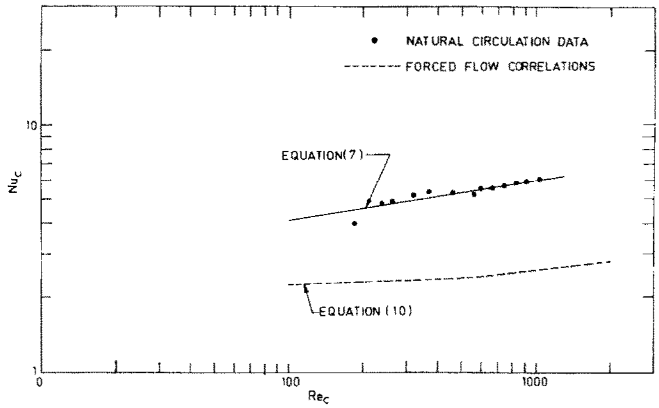

FIG. 3. Correlation for Nusselt number for the cooler.

correlations (9) and (12). The figure clearly shows that both $K_{eff,cor}$ and $K_{eff,f}$ underpredict the natural circulation data, although the latter is in good agreement at low values of Re_c (< 300). Poor agreement of $K_{eff,cor}$ is already expected as the lengths of the individual segments are not large enough for fully developed flow to be established. The $K_{eff,f}$ on the other hand fails to predict the natural circulation data because of the failure to account for the effects of secondary flows under natural circulation conditions that become particularly important at large Reynolds numbers.

It is therefore important to conclude that for accurate predictions of loop mass flow rates, and more importantly of the fluid and heater temperatures, accurate prescription of K_{eff} under natural circulation conditions is needed. However, there does not exist any independent correlation that can predict $K_{eff,nc}$ as yet. However, by examining natural circulation data from different loops, it may be possible to develop a generalized correlation applicable to all loops. The basis for such a correlation and the correlation itself are presented in Section 4.

Such an approach to the development of the correlation for natural circulation conditions is desirable because of the convenience it offers in the evaluation of important parameters by the simple equation (1). The alternative is to solve complete three-dimensional (3-D) Navier–Stokes equations along with the 3-D energy equation to predict the parameters of interest. This approach has been followed for a toroidal loop of uniform cross-section by Lavine [32]. For complex loop geometries of nuclear reactors, this approach is of course, too cumbersome.

Figure 3 plots both equations (10) for $Nu_{c,cor}$ and (7) for $Nu_{c,nc}$ along with the experimental data obtained under natural circulation conditions. It is seen that the conventional correlations yield $Nu_{c,cor}$ that grossly underpredicts the natural circulation data. This is attributed to the presence of buoyancy and curvature generated secondary flows in the U-tube cooler which increase the magnitude of the heat transfer coefficient on the primary side. Similarly correlations (11) for $Nu_{h,cor}$ and (8) for $Nu_{h,nc}$ along with the natural circulation experimental data are presented in Fig. 4. Again the natural circulation data are not correlated by the correlations found in the literature due to the presence of secondary flows under natural circulation conditions.

3.3. *Closure*

Thus overall it can be said that neither the K_{eff}, Nu_c and Nu_h obtained from the usual correlations can predict the experimental data under natural circulation conditions in the present experimental set up, except at very low Reynolds numbers. In the case of K_{eff}, even the experimentally determined correlation with forced flow fails to predict the natural circulation K_{eff} data. It is obvious then that correlations that account for the effect of buoyancy generated secondary flows are needed. Such correlations must inevitably be loop specific, as has been the experience of several previous investigators [13, 23].

In the next section, however, it is demonstrated that a non-loop specific generalized correlation for K_{eff} can in fact be developed, although the same cannot be extended to Nu_c and Nu_h which depend on the local geometries of the heater and the cooler in different loops.

4. GENERALIZED CORRELATION FOR K_{eff}

4.1. *The purpose*

Most of the reported experimental data on natural circulation loops are presented either in dimensional form or in terms of non-dimensional groups which are loop specific. This makes it difficult to compare data from different loops and to extend data from small-scale to large-scale loops. Therefore, the available experimental data from various loops are re-examined in order to arrive at some generalized dimensionless groups applicable for all loops. Before so doing, however, the different dimensionless groups so far proposed for natural circulation loops are examined in the next sub-section.

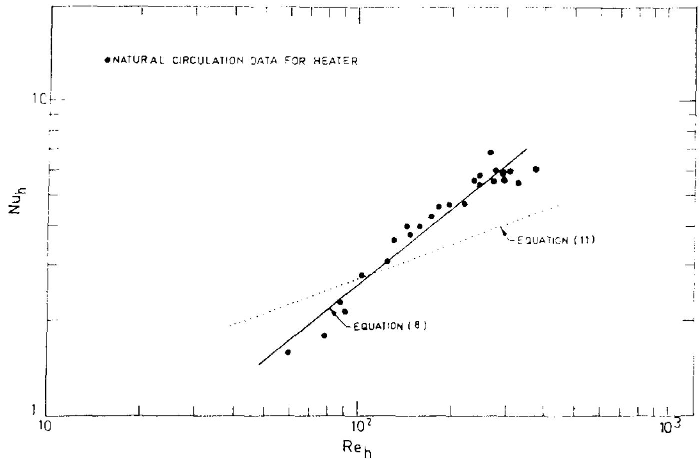

FIG. 4. Correlation for Nusselt number for the heater.

4.2. *Different dimensionless groups*

An important attribute of a correlation for K_{eff} must be that it is related to dimensionless groups that comprise of only those quantities that are externally controlled. Such quantities in natural circulation loops are: Q_h, W_s, C_{p_s}, T_{si} and the geometrical quantities such as the segmental lengths and diameters. None of the temperatures such as T_{hl}, T_{cl}, $\bar{T}_h$ (or their differences) and flow rate W should be present in the dimensionless groups as these are dependent variables. This requirement also suggests that the fluid properties that are necessarily required in the formation of the dimensionless groups are also defined in relation to some known reference temperature and are not dependent on the loop temperatures. None of the dimensionless groups so far proposed really meet these requirements as is shown below.

In ref. [33], equation (1) is rewritten as

$$K_{eff} = 2Gr''_m/Re_c^2 \tag{13}$$

where

$$Gr''_m = D_c^2 Z_m \rho_m^2 \beta g \Delta T_h/\mu^2;$$

$$Re_c = D_c W/A_c\mu \text{ and } \Delta T_h = T_{hl} - T_{cl}.$$

A similar definition is also used by Hallinan and Viskanta [11]. By replacing W with $Q_h/C_p\Delta T_h$, Lapin [6] has represented K_{eff} as

$$K_{eff} = p(\pi^2/16)(Gr''\,Pr^2/(Nu'')^2)(Z_m/D_c) \tag{14}$$

where

$$Nu'' = Q_h/(kD_c\Delta T_h);\quad Gr = D_c^3\rho^2\beta g\Delta T_h/\mu^2;$$

$$Pr = C_p\mu/k.$$

Note that equations (13) and (14) retain W and ΔT_h and hence cannot qualify for non-loop-specific prescription of K_{eff}. A straightforward reorganization of equation (13) would however suggest that K_{eff} can be represented as

$$K_{eff} = p\,Gr_{m_c}/Re_c^3 \tag{15}$$

where

$$Gr_{m_c} = D_c^3\rho_m^2\beta g\Delta T_r/\mu^2 \tag{16}$$

and

$$\Delta T_r = Q_h Z_m/(\mu A_c C_p). \tag{17}$$

Note that a reference temperature difference ΔT_r is now newly introduced. The purpose of introducing ΔT_r is that a Grashof number Gr_{m_c} representing a characteristic velocity $(\beta g D_c \Delta T_r)^{1/2}$, can now be calculated independently.

It was shown in Section 3.2 that $K_{eff,nc}$ for natural circulation can be represented in a generalized form as

$$K_{eff} = a/Re_c^b. \tag{18}$$

Equating equation (18) with equation (15), we obtain

$$Re_c = [p\,Gr_{m_c}/a]^{(1/3-b)} \tag{19a}$$

or

$$Re_c = B(Gr_{m_c})^{1/n} \tag{19b}$$

where B and n are loop-specific constants. Based on forced flow correlations n can take values between 2 (for laminar flow with $b = 1$) and 2.75 (for turbulent flow with $b = 0.25$) whereas no such limits can be specified for the constant B. Substituting equation (19b) in equation (15), K_{eff} can be written as

$$K_{eff} = (p/B^3)[Gr_{m_c}]^{1-3/n}. \tag{20}$$

It is thus possible to represent K_{eff} in terms of independently calculable Gr_{m_c}, provided B and n are known. The advantage derived from development of equation (20) is that both Re_c and Gr_{m_c} can now be evaluated from the published data; and hence B and n can be determined for different loops.

4.3. *Relationship between* Gr_{m_c} *and* Re_c

Creveling *et al.* [13] and Bau and Torrance [23] in their experiments with a toroidal loop and an open loop, respectively, have plotted all their data in the form of a relationship between Gr_{m_c} and Re_c rather than invoking a relationship between K_{eff} and Gr_{m_c} in the form of equation (20). For example, Creveling *et al.* [13] present their data in the form of

$$(Nu\,Gr/Pr)R/r = C_1(Re_c)^m \quad (21)$$

where $Nu = 2rh/k$, $Gr = (2r)^3\rho^2\beta g(T_b - T_w)/\mu^2$, R is the radius of the torus, r the radius of the tube forming the torus and $(\bar{T}_b - \bar{T}_w)$ the mean fluid temperature difference in the cooler.

That equation (21) represents a relationship between Gr_{m_c} and Re_c can be discerned if it is recognized that

$$Gr_{m_c} = (Nu\,Gr/Pr)(A_{hc}/A_c)(Z_m/D_c).$$

Hence Creveling *et al.*'s correlation can be written in the form of equation (19b) as

$$Re_c = [(A_c/A_{hc})(D_c/Z_m)(R/r)/C_1]^{1/m}(Gr_{m_c})^{1/m}. \quad (21a)$$

The non-dimensional parameters proposed in the recent paper by Huang and Zelaya [12] for a rectangular uniform diameter loop are almost identical to those used by Creveling *et al.* [13] except that an equivalent length to account for the effect of different openings of the control valve in the loop has also been introduced. Similarly, Bau and Torrance [23] represent their data as

$$Re_c = C_1(Q^*)^{1/m} \quad (22)$$

where

$$Q^* = D^2\rho^2\beta g Q_h Z_m/(L_t C_p \mu^3)$$

and L_t is the total length of the loop. But it is easy to discern that

$$Gr_{m_c} = (4L_t/\pi D)Q^*$$

and hence correlation (22) can be written as

$$Re_c = C_1[\pi D/4L_t]^{1/m}(Gr_{m_c})^{1/m} \quad (22a)$$

Thus equations (21a) and (22a) confirm our proposition that a direct relationship between Re_c and Gr_{m_c} must exist for different loops. With this evidence, the raw data from eight experimental investigations [9, 16, 17, 19, 20, 23, 24, 34] and the present data were analysed and values of Re_c with the corresponding Gr_{m_c} were derived for each investigation. Experimental data of refs. [16, 17, 23, 24, 34] and the present data showed that Gr_{m_c} values in their experiments were in the range $2\times10^8 < Gr_{m_c} < 2\times10^{12}$ where as the data of refs. [9, 19, 20] showed their Gr_{m_c} values were in the range $10^{13} < Gr_{m_c} < 2\times10^{16}$. Hence Re_c vs Gr_{m_c} for the two different ranges of Gr_{m_c} are plotted separately in Figs. 5 and 6, respectively.

The figures show that although the loops used by different investigators differ widely in their geometry (see Table 2 for their details), all the data including the data from the present loop are found to be remarkably parallel suggesting a universal value of n in equation (19b), with different values of B. To be precise, the values of n found are

$$n = 2.365 \text{ for } 2\times10^8 < Gr_m < 2\times10^{12} \quad (23)$$

and

$$n = 2.77 \text{ for } 10^{13} < Gr_m < 2\times10^{16}. \quad (24)$$

It may be noted that Creveling *et al.* [13] and Bau and Torrance [23] indirectly correlated their data with $n = 2.56$ $(10^{10} < Gr_{m_c} < 3\times10^{11})$ and $n = 2.427$ $(4\times10^8 < Gr_{m_c} < 3\times10^{10})$, respectively. Further, the data of Davis and Morris [27] (whose raw data are not available and hence not considered here) for a rotating closed loop also indirectly implies $n = 2.45$ $(2\times10^8 < Gr_{m_c} < 2\times10^{10})$, thus providing further evidence to equation (23). In nuclear reactors, where Gr_m is typically greater than 10^{16}, turbulent flow conditions are expected and $n = 2.75$ (turbulent forced flow) often used in such calculations is adequate as shown by equation (24).

In our search for a generalized prescription for K_{eff}, further investigation must be directed towards collapsing the different curves on a single curve, i.e. providing a basis for generalizing the values of B found for different loops. It is to this matter we now turn.

4.4. *The generalized correlation*

The characteristic dimensions used in the definition of Gr_{m_c} and Re_c have been those of the cooler, i.e. D_c and A_c. The cooler, of course, represents only one segment in any loop and loss in generality of the relationship between Re and Gr_m can result from use of D_c and A_c. Therefore, the Re and Gr_m were redefined as

$$Re = D_e W/(A_e \mu) \quad (25)$$

$$Gr_m = D_e^3\rho^2\beta g\Delta T_r/\mu^2 \quad (26)$$

where

$$\Delta T_r = Q_h Z_m/(A_e \mu C_p). \quad (27)$$

D_e and A_e are the equivalent diameter and the equivalent cross-sectional area of the loop, respectively, and are defined as

$$D_e = 4\times(\text{Loop volume})/(\text{Wetted surface})$$

$$= 4\sum_i A_i L_i \Big/ \sum_i P_i L_i \quad (28)$$

and

$$A_e = (\text{Loop volume})/(\text{Total loop length})$$

$$= (1/L_t)\sum_i A_i L_i \quad (29)$$

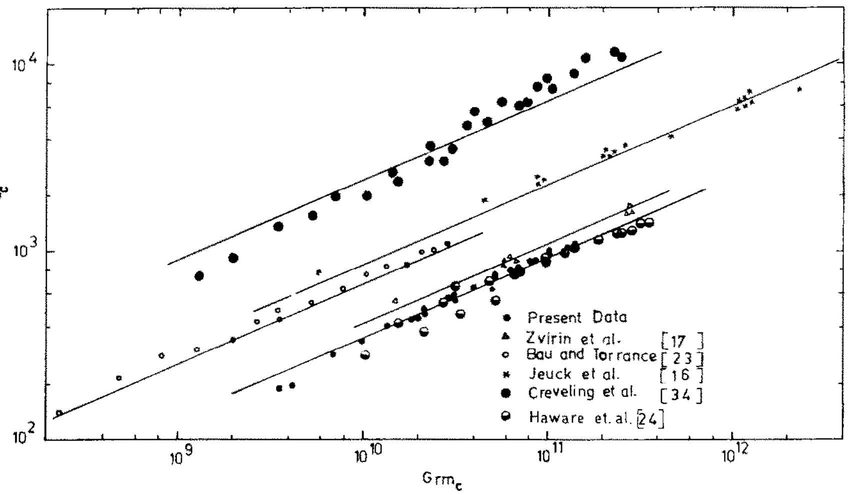

FIG. 5. Natural circulation data from various loops.

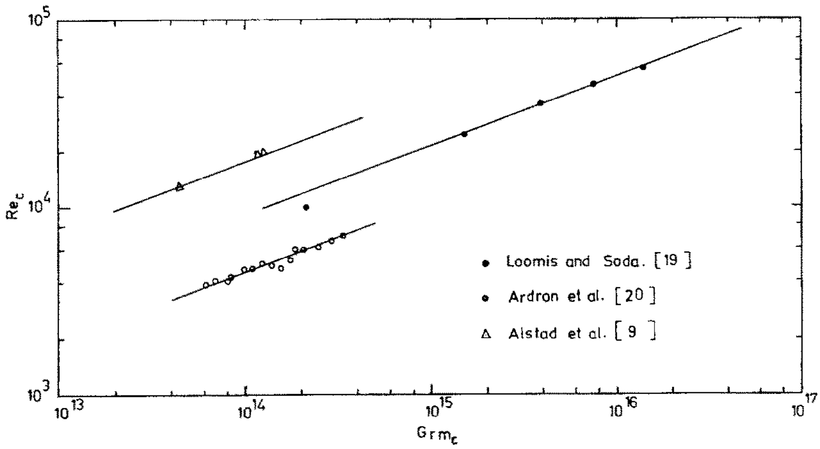

FIG. 6. Natural circulation data from various loops.

Table 2. Geometric details of loops considered in Figs. 5 and 6

Serial No.	Author	Type of loop	Features	Remarks
1	Creveling [34]	Toroidal	Uniform diameter	High heat losses
2	Bau and Torrance [23]	Open loop	Uniform diameter	—
3	Haware *et al.* [24]	Open loop	Uniform diameter	Experimental data for three elevations are presented
4	Zvirin *et al.* [17]	Loop relevant to PWR	Variable diameter	Single-loop and two-loop data are presented
5	Jeuck *et al.* [16]	Loop relevant to PWR	Variable diameter	Single-, two-, three- and four-loop data are presented
6	Loomis and Soda [19]	Loop relevant to PWR	Variable diameter	Experiments at high pressure and temperature with compensation for heat loss
7	Ardron *et al.* [20]	Figure-of-eight	Variable diameter	Experiments at high pressure and temperature
8	Alstad *et al.* [9]	Rectangular	Variable diameter	Data generated with two different heat exchangers
9	Present data	Figure-of-eight	Variable diameter	Heat losses less than 12%

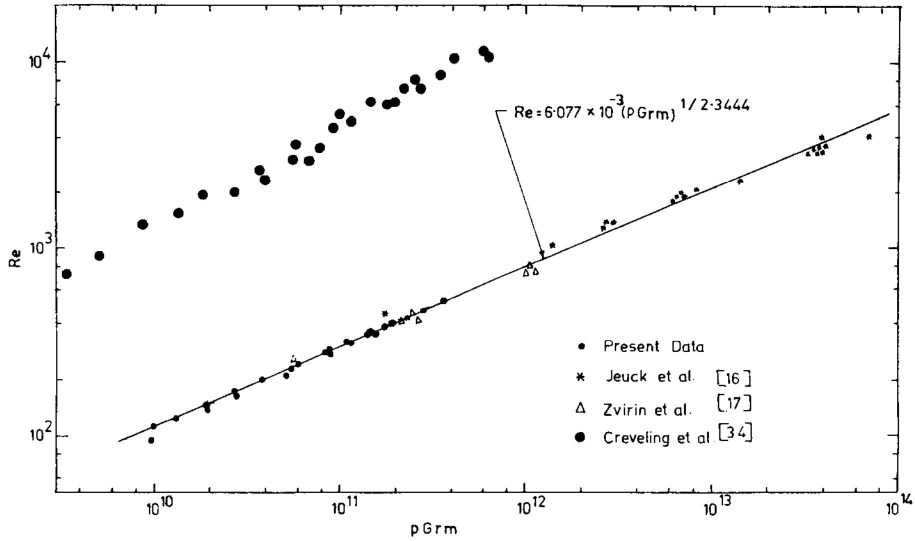

FIG. 7. Generalized correlation for natural circulation loops.

where A_i, P_i and L_i are the flow area, wetted perimeter and length, respectively, of the ith segment. For identical parallel loop systems the loop volume, wetted surface and equivalent flow area are defined by the following equations:

Loop volume, $V = \sum_i V_i W_i / W$

Wetted surface, $S = \sum_i S_i W_i / W$

Mean flow area, $A_e = m(A_e)_{\text{for single loop}}$

where m is the number of parallel loops. With these definitions, the hydraulic diameter remains the same for the single-loop and parallel-loop systems considered in refs. [16, 17].

Using these new definitions, Re and Gr_m were recalculated for all loops except those of refs. [19, 20, 23, 24]. These latter references were excluded as complete data on their geometry were unavailable. These data also pertained to $Gr_m > 10^{13}$, hence data corresponding to the Gr_m range of equation (23) alone is considered. The loops considered, however, still represent seven geometrically dissimilar configurations (see Table 2).

Now since p is a known constant that differs from loop to loop, data were replotted as Re vs $(p\,Gr_m)$ and are shown in Fig. 7. It is seen that all data except the data of Creveling [34] are in excellent agreement. Further examination of Creveling's toroidal loop data however showed that the data were obtained with heat losses that were as high as 50% of the heater power. This would introduce error in the evaluated Gr_m and Re (through false estimation of W) and thus disagreement with the general trend can be expected.

The generalized relationship can now be expressed as

$$Re = 6.077 \times 10^{-3}(p\,Gr_m)^{(1/2.3444)} \tag{30}$$

and hence K_{eff} can now be evaluated as

$$K_{\text{eff}} = 1.57 \times 10^5 / Re^{0.6556};$$

$$\text{for } 6 \times 10^9 < p\,Gr_m < 10^{14} \tag{31}$$

$$K_{\text{eff}} = 4.455 \times 10^6 (p\,Gr_m)^{-0.2797};$$

$$\text{for } 6 \times 10^9 < p\,Gr_m < 10^{14}. \tag{31a}$$

Thus our aim of developing an independent, non-loop-specific generalized correlation for K_{eff} is successfully achieved. The probable reason for achieving collapse of data from different loops on a single curve when Gr_m is defined, based on equivalent diameter and equivalent cross-sectional area, may be that the secondary flows under natural circulation conditions play the same role as is played by the turbulence driven secondary flows in non-circular ducts, where the hydraulic diameter concept has been found to be applicable.

Note that in a transient analysis, if a quasi-static approximation is made then equation (31) is still appropriate with Re calculated instantaneously.

4.5. *Closure*

By defining equivalent cross-sectional area and diameter, a basis has been found for obtaining a generalized correlation for K_{eff} that can be applied to any loop with reasonable confidence in the range of Gr_m values quoted in equation (31).

In nuclear reactors natural circulation occurs at $Gr_m > 10^{16}$, and highly turbulent conditions prevail. It cannot be claimed that equations (30) and (31)

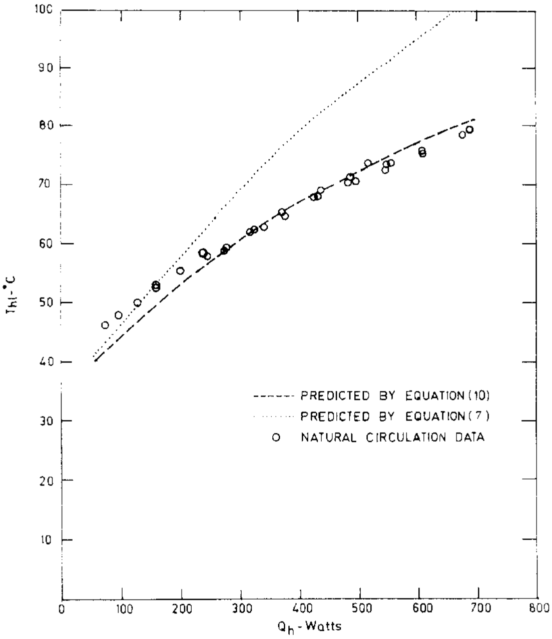

FIG. 8. Predicted and measured hot leg temperature for the present loop.

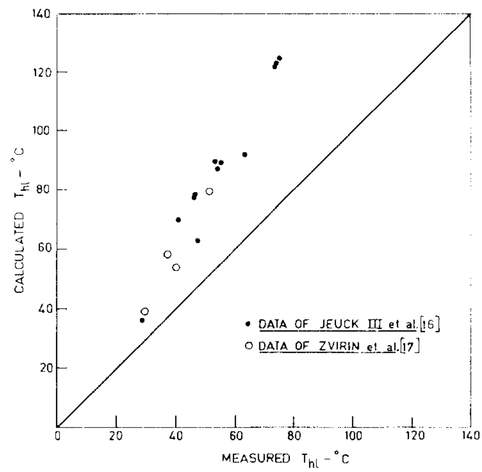

FIG. 9. Measured and predicted hot leg temperatures.

are directly applicable to this situation. However, the general form of the equations can still be valid and can be used for scaling of actual reactor loops; and the present deductions suggest that, apart from maintaining geometric similarity, the similarity of Gr_m should also be maintained if realistic results are to be obtained. This is an important result, since in the past studies, similarity of Reynolds number has been maintained (e.g. ref. [16]) or in ref. [28], simulation studies have been carried out by maintaining a 1 : 1 ratio in elevations.

In Section 5 below, the ability of correlation (30) to predict heater temperature T_h and hot leg temperature T_{hl} (and hence T_{cl}) is tested with reference to the present experimental data as well as some published data from other loops.

5. TESTING OF THE GENERALIZED CORRELATION FOR K_{eff}

5.1. *Prediction of* T_{hl}

The T_{hl} data from the present loop are plotted against Q_h in Fig. 8 with W evaluated from equation (30). Two correlations for Nu_c are used, i.e. equations (7) and (10). From the figure it is found that $Nu_{c,nc}$ predicts the data well. Due to the wide difference between $Nu_{c,nc}$ and $Nu_{c,cor}$ as shown in Fig. 3, T_{hl} data are overpredicted by the use of the latter.

Measured and predicted hot leg temperatures for the other two loops [16, 17] are presented in Fig. 9. Again in both cases W is evaluated from equation (30) and $Nu_{c,cor}$ has been used which as before gives conservative prediction. The $Nu_{c,nc}$ values for these loops are, however, not available.

5.2. *Prediction of* $\bar{T}_h$

Figure 10 shows the presently measured and predicted average heater temperature using equations (11) and (8) for Nu_h and equation (30) for W. Again, the heater temperature is conservatively predicted by the conventional correlation (i.e. $Nu_{h,cor}$), whereas the natural circulation prediction (i.e. by using $Nu_{h,nc}$) agrees well with the data. Unfortunately, no published data are available on heater temperatures in other loops to extend this comparison further.

Thus the generalized correlation for K_{eff} alone is not sufficient to predict the loop temperatures well and it is necessary to develop correlations applicable to natural circulation conditions for the Nusselt number at the cooler as well as at the heater.

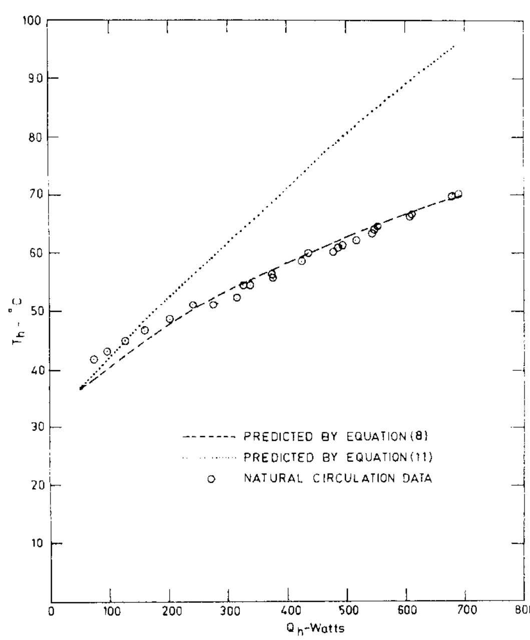

FIG. 10. Predicted and measured average heater temperature.

6. CONCLUSIONS

The following are the conclusions of this paper.

(1) For the same Reynolds number, the magnitude of the measured effective pressure loss coefficient $K_{eff,nc}$ under natural circulation conditions exceeds the magnitude of the loss coefficient $K_{eff,f}$ measured under forced flow conditions by as much as 30%. This is due to the presence of cross-sectional secondary flows induced by buoyancy.

(2) The measured natural circulation overall Nusselt number for the cooler, $Nu_{c,nc}$, greatly exceeds the Nu_c values evaluated from published forced flow correlations. The same comment applies to the Nusselt number in the heater. This deviation is again attributed to the presence of secondary flows during natural circulation.

(3) A generalized correlation for K_{eff} applicable to several loops is successfully derived in terms of a newly defined Grashof number Gr_m that can be independently calculated from the known operating conditions and the geometry of the loop. In this sense, claims to universality can be made. An added attribute of the correlation is that it does not use any of the dependent variables and as such the usual iterative calculations necessary for prediction of the mass flow rate are eliminated. The new generalized correlation has shown that apart from geometric similarity, similarity of Gr_m should be maintained in scaling of prototype loops.

(4) The predictions of T_{hl} and $\bar{T}_h$ from the present as well as other loops has shown that it is necessary to specify accurately K_{eff}, Nu_c and N_h for natural circulation conditions to obtain reasonable predictions of the temperatures. However, accurate prediction of flow rate requires only K_{eff} to be prescribed accurately.

Acknowledgements—Acknowledgements are due to the authors of refs. [11, 13, 16–19, 23, 24] for providing raw data of their experimental loops.

REFERENCES

1. D. Japikse, Advances in thermosyphon technology. In *Advances in Heat Transfer* (Edited by T. F. Irvine, Jr. and J. P. Hartnett), Vol. 9, pp. 1–111. Academic Press, New York (1973).
2. Y. Zvirin, A review of natural circulation loops in pressurised water reactors and other systems, *Nucl. Engng Des.* **67**, 203–225 (1981).
3. A. Mertol and R. Greif, Review of thermosyphon solar water heaters. In *Solar Energy Utilization: Fundamentals and Applications* (Edited by H. Yuncu). Martinus Nijhoff, The Netherlands (1987).
4. A. Mertol and R. Greif, A review of natural circulation loops. In *Natural Convection: Fundamentals and Applications* (Edited by S. Kakac, W. Aung and R. Viskanta), pp. 1033–1071. Hemisphere, New York (1985).
5. R. Greif, Natural circulation loops, *J. Heat Transfer* **110**, 1243–1258 (1988).
6. Y. D. Lapin, Heat transfer in communicating channels under conditions of free convection, *Thermal Engng* **16**, 94–97 (1969).
7. J. Madejski and J. Mikielewicz, Liquid fin—a new device for heat transfer equipment, *Int. J. Heat Mass Transfer* **14**, 354–363 (1971).
8. D. C. Hamilton, F. E. Lynch and L. D. Palmer, The nature of the flow of ordinary fluids in a thermal convection harp, ORNL-1624 (1954).
9. C. D. Alstad, H. S. Isbin, N. R. Amundson and J. P. Silvers, The transient behaviour of single-phase natural circulation water loop systems, ANL-5409 (1956).
10. C. P. Agarwal, S. S. Alam and N. Gopalakrishna, Heat transfer studies in a vertical tube of a closed-loop thermosyphon, *Trans. IIChE* **21**, 37–44 (1979).
11. K. P. Hallinan and R. Viskanta, Heat transfer from a vertical tube bundle under natural circulation conditions, *Int. J. Heat Fluid Flow* **6**, 256–264 (1985).
12. B. J. Huang and R. Zelaya, Heat transfer behaviour of a rectangular thermosyphon loop, *J. Heat Transfer* **110**, 487–493 (1988).
13. H. F. Creveling, J. F. De Paz, J. Y. Baladi and R. J. Schoenhals, Stability characteristics of a single-phase free convection loop, *J. Fluid Mech.* **67**, 65–84 (1975).
14. P. S. Damerell and R. J. Schoenhals, Flow in a toroidal thermosyphon with angular displacement of heated and cooled sections, *J. Heat Transfer* **101**, 672–676 (1979).
15. M. Sen, D. A. Pruzan and K. E. Torrance, Analytical and experimental study of steady-state convection in a double-loop thermosyphon, *Int. J. Heat Mass Transfer* **31**, 709–722 (1988).
16. P. Jeuck III, L. Lennert and R. L. Kiang, Single-phase natural circulation experiments on small-break accident heat removal, EPRI NP-2006 (1981).
17. Y. Zvirin, P. R. Jeuck III, C. W. Sullivan and R. B. Duffey, Experimental and analytical investigation of a natural circulation system with parallel loops, *J. Heat Transfer* **103**, 645–652 (1981).
18. P. R. Jeuck III and R. L. Kiang, Natural circulation experiments in a UTSG four-loop test facility, EPRI NP-2615 (1982).
19. G. G. Loomis and K. Soda, Results of the semi-scale MOD-2A natural circulation experiments, NUREG/CR-2335 and EGG-2200, Idaho National Engineering Laboratory (1982).
20. K. H. Ardron, V. S. Krishnan, G. R. McGee, J. W. D. Anderson and E. H. Hawley, Two-phase natural circulation experiments in a pressurised water loop with figure-of-eight symmetry. In *Experimental and Modelling Aspects of Small-break LOCA, Proc. Specialists' Meeting*, IAEA, Budapest, Hungary, 3–7 October (1983).
21. R. M. Mandl and P. A. Weiss, PKL tests on energy transfer mechanisms during small-break LOCAs, *Nucl. Safety* **23**, 148–154 (1982).
22. P. K. Vijayan, V. Venkat Raj, S. K. Mehta and A. W. Date, Phenomenological investigations on natural circulation in a loop relevant to a PHWR, ASME Paper No. 85-WA/HT-17 (1985).
23. H. H. Bau and K. E. Torrance, Transient and steady behaviour of an open, symmetrically heated, free convection loop, *Int. J. Heat Mass Transfer* **24**, 597–609 (1981).
24. S. K. Haware, R. B. Grover and V. Venkat Raj, Experimental investigation into natural convection heat transfer in an open-loop thermosyphon with horizontal tubes, HMT-D2-83, VIIth Natn. Heat and Mass Transfer Conf., Indian Institute of Technology, Kharagpur (1983).
25. J. C. Chato, Natural convection flows in parallel-channel systems, *J. Heat Transfer* **85**, 339–345 (1963).
26. K. S. Ong, A finite-difference method to evaluate the thermal performance of a solar water heater, *Solar Energy* **16**, 137–147 (1974).
27. T. H. Davis and W. D. Morris, Heat transfer characteristics of a closed loop rotating thermosyphon, *Proc. 3rd Int. Heat Transfer Conf.*, Chicago, Vol. 2, pp. 172–181 (1966).

28. G. G. Loomis and K. Soda, Natural circulation in an experimental facility scaled from a pressurised water reactor, Paper No. NR-16, *Proc. Seventh Int. Heat Transfer Conf.* (1982).
29. R. H. Perry and C. H. Chilton (Editors), *Chemical Engineers' Handbook*, 5th Edn. McGraw-Hill/KogaKusha Ltd., Tokyo (1973).
30. I. E. Idel' Chik, *Handbook of Hydraulic Resistances*. Dept. NTIS (1960).
31. C. Y. Chen, G. A. Hawkins and H. I. Solberg, Heat transfer in annuli, *Trans. ASME* **68**, 99–106 (1946).
32. A. S. Lavine, R. Greif and J. A. C. Humphrey, A three-dimensional analysis of natural convection in a toroidal loop—the effect of Grashof number, *Int. J. Heat Mass Transfer* **30**, 251–261 (1987).
33. P. K. Vijayan, V. Venkat Raj, S. K. Mehta and A. W. Date, Investigations on natural circulation in a figure-of-eight loop, HMT-B-10-85, *Proc. VIIIth Natn. Heat and Mass Transfer Conf.*, Andhra University, Vishakhapatnam, 29–31 December (1985).
34. H. F. Creveling, Ph.D. Thesis, Purdue University (1964).

SUR LES PERFORMANCES DES BOUCLES DE CIRCULATIONS PERMANENTES NATURELLES

Résumé—On rapporte une comparaison entre les données de circulations naturelles et forcées dans des boucles en forme de huit relatives à des réacteurs à eau lourde. On montre que le frottement et le transfert de chaleur sont affectés par la présence d'écoulements secondaires induits par le flottement dans des conditions de circulation naturelle permanente. Quelques propositions antérieures sur le coefficient de perte de charge sont réservées et une formule générale est proposée. Celle-ci prédit avec succès les résultats expérimentaux de trois boucles différentes. Les données expérimentales sont relatives à sept configurations géométriques de ces trois boucles.

DAS VERHALTEN VON NATURUMLAUFSYSTEMEN IN STATIONÄREN BETRIEBSZUSTÄNDEN

Zusammenfassung—Zwangsumlauf- und Naturumlaufdaten eines verschlungenen, achtförmigen Kreislaufes werden verglichen. Kreisläufe dieser Art sind in Druckwasserreaktoren mit schwerem Wasser zu finden. Es zeigt sich, daß Reibung und Wärmeübergang bei stationärem Naturumlauf durch auftriebsbedingte Sekundärströmungen beeinflußt werden. Mehrere frühere Vorschläge, den Koeffizienten für den hydraulischen Gesamtdruckverlust zu korrelieren, werden überprüft und eine verallgemeinerte Korrelation, die von der Geometrie des verwendeten Kreislaufes unabhängig ist, wird vorgestellt. Mit dieser Korrelation können die Versuchsdaten von drei verschiedenen Kreislaufsystemen gut wiedergegeben werden. Die Versuchsdaten wurden mit sieben unterschiedlichen geometrischen Anordnungen dieser drei Kreisläufe bestimmt.

СТАЦИОНАРНАЯ ХАРАКТЕРИСТИКА КОНТУРА ЕСТЕСТВЕННОЙ ЦИРКУЛЯЦИИ

Аннотация—Проведено сравнение данных по естественной и вынужденной циркуляции в контуре в форме восьмерки, характерном для реактора на тяжелой воде. Показано, что как трение, так и теплоперенос подвержены воздействию обусловленных подъемной силой свободноконвективных вторичных течений в условиях стационарной естественной циркуляции. Рассмотрены некоторые предыдущие предложения по корреляции коэффициента общих гидравлических потерь, и предложено обобщающее соотношение, пригодное не только для данного контура. Это соотношение позволяет успешно прогнозировать экспериментальные данные для трех различных контуров, которые получены при семи разных геометрических конфигурациях трех рассматриваемых контуров.